

12-2005

Lattice Quantum Algorithm for the Schrodinger Wave Equation in 2+1 Dimensions With a Demonstration by Modeling Soliton Instabilities

Jeffrey Yepez

George Vahala

Linda L. Vahala

Old Dominion University, lvahala@odu.edu

Follow this and additional works at: https://digitalcommons.odu.edu/ece_fac_pubs

 Part of the [Computational Engineering Commons](#), [Partial Differential Equations Commons](#), and the [Quantum Physics Commons](#)

Repository Citation

Yepez, Jeffrey; Vahala, George; and Vahala, Linda L., "Lattice Quantum Algorithm for the Schrodinger Wave Equation in 2+1 Dimensions With a Demonstration by Modeling Soliton Instabilities" (2005). *Electrical & Computer Engineering Faculty Publications*. 44.

https://digitalcommons.odu.edu/ece_fac_pubs/44

Original Publication Citation

Yepez, J., Vahala, G., & Vahala, L. (2005). Lattice quantum algorithm for the Schrödinger wave equation in 2+1 dimensions with a demonstration by modeling soliton instabilities. *Quantum Information Processing*, 4(6), 457-469. doi: 10.1007/s11128-005-0008-8

Lattice Quantum Algorithm for the Schrödinger Wave Equation in 2+1 Dimensions with a Demonstration by Modeling Soliton Instabilities

Jeffrey Yepetz,^{1,4} George Vahala,² and Linda Vahala³

Received July 8, 2005; accepted December 5, 2005; published online February 24, 2006

A lattice-based quantum algorithm is presented to model the non-linear Schrödinger-like equations in $2 + 1$ dimensions. In this lattice-based model, using only 2 qubits per node, a sequence of unitary collide (qubit-qubit interaction) and stream (qubit translation) operators locally evolve a discrete field of probability amplitudes that in the long-wavelength limit accurately approximates a non-relativistic scalar wave function. The collision operator locally entangles pairs of qubits followed by a streaming operator that spreads the entanglement throughout the two dimensional lattice. The quantum algorithmic scheme employs a non-linear potential that is proportional to the moduli square of the wave function. The model is tested on the transverse modulation instability of a one dimensional soliton wave train, both in its linear and non-linear stages. In the integrable cases where analytical solutions are available, the numerical predictions are in excellent agreement with the theory.

KEY WORDS: Non-linear Schrödinger wave equation; quantum algorithm; soliton dynamics; non-linear quantum mechanical instability; quantum computing; computational physics.

PACS: 03.67.Lx; 05.45.Yv; 02.60.Cb.

1. INTRODUCTION

The non-linear Schrödinger (NLS) equation is one of the most basic equations of non-linear physics. Its salient feature is that it admits soliton solutions by exact integration. Hence, it plays a vital role in weakly non-linear systems

¹ Air Force Research Laboratory, Hanscom Field, Bedford, MA 01731, USA.

² Department of Physics, William & Mary, Williamsburg, VA 23187, USA.

³ College of Engineering & Technology, Old Dominion University, Norfolk, VA 23529, USA.

⁴ To whom correspondence should be addressed. E-mail: jeffrey.yepetz@hanscom.af.mil, URL: <http://qubit.plh.af.mil>

with the dispersion relation dependent on the wave amplitude. The NLS equation is pivotal in non-linear optics,⁽¹⁾ plasma physics⁽²⁾ as well as in ideas for information transfer in optical computers.^(3,4) In 1+1 dimensions, both the focusing and defocusing NLS equations are exactly integrable and exhibit soliton solutions. Here, we develop and test a quantum lattice representation of the (focusing) NLS equation in 2+1 dimensions

$$i\partial_t\psi + \partial_{xx}\psi + \partial_{yy}\psi + 2|\psi|^2\psi = 0. \quad (1)$$

building on our previous quantum lattice representations of the Schrödinger wave equation,⁽⁵⁾ NLS equation⁽⁶⁾ and the vector Manakov system⁽⁷⁾ in 1+1 dimensions and the Dirac equation in 3+1 dimensions.⁽⁸⁾ In particular, we shall consider the transverse modulational instability of the one-dimensional soliton wave train solution $\psi_\circ(x, t)$ of (1).

In the quantum lattice algorithm for the Schrödinger equation, at each spatial node, the wave function is represented by the interference sum of probability amplitudes of the upper excited state of each qubit. In the quantum algorithm for the NLS equation in 1+1 dimensions, 2 qubits per node are used, and collisional interaction is induced by the unitary \sqrt{SWAP} quantum logic gate. The \sqrt{SWAP} quantum gate has been implemented experimentally using 2 qubits per computational node in a quantum lattice gas model of the diffusion equation.^(9,11) This entanglement is then spread throughout the lattice by the unitary streaming operator, which is real. In extending the algorithm to 2+1 dimensions, still only 2 qubits per node are required and the \sqrt{SWAP} still represents local qubit–qubit interactions. If implemented on a platform using future quantum information processing device technology, the quantum algorithm presented here is suited for a type-I quantum computer architecture, as described in this Quantum Computation for Physical Modelling (QCPM) special issue in Section A of,⁽⁸⁾ but with local non-linear interactions inherent in the quantum device.

2. QUBIT REPRESENTATION FOR THE NLS WAVE FUNCTION IN 2+1 DIMENSIONS

We discretize the single-particle wave function over a two dimensional square Bravais lattice (the wave function is defined only on a spacetime lattice) where 2 qubits are used at each lattice node to encode the local value of the wave function at that node. Let L denote the number of lattice nodes along an orthogonal direction and let i and j be integer valued spatial indices ranging from 1 up to L . Then, at lattice node (i, j) one defines a position basis ket $|x_{ij}\rangle$. The discretized single-particle wave

function ket $|\psi\rangle$ is modelled by a sum over all possible ways the particle can be located on the lattice sites:

$$|\psi\rangle = \sum_{i,j=0}^{L-1} \gamma^{ij} |x_{ij}\rangle, \quad (2)$$

where the (complex) probability amplitude for each possibility is $\gamma^{ij} \equiv \langle x^{ij} | \psi \rangle$.

The two qubit kets for each lattice node are denoted by $|q_0^{ij}\rangle$ and $|q_1^{ij}\rangle$ with each qubit having the standard two-level representation

$$|q_a^{ij}\rangle = \alpha_a^{ij} |0\rangle + \beta_a^{ij} |1\rangle, \quad (3)$$

with normalization $|\alpha_a^{ij}|^2 + |\beta_a^{ij}|^2 = 1$ for $a = 0, 1$ at spatial site (i, j) . In particular, the quantum particle is said to occupy the a th local state at position x_{ij} when $\beta_a^{ij} = 1$, while the a th local state at x_{ij} is empty when $\beta_a^{ij} = 0$. For each position ket there are four basis states in the number representation:

$$\begin{array}{ll} |q_0^{11} q_1^{11}\rangle \cdots \underbrace{|11\rangle}_{x_{ij}} \cdots |q_0^{LL} q_1^{LL}\rangle & \text{doubly occupied at } x_{ij} \\ |q_0^{11} q_1^{11}\rangle \cdots \underbrace{|10\rangle}_{x_{ij}} \cdots |q_0^{LL} q_1^{LL}\rangle & \text{spin-up at } x_{ij} \\ |q_0^{11} q_1^{11}\rangle \cdots \underbrace{|01\rangle}_{x_{ij}} \cdots |q_0^{LL} q_1^{LL}\rangle & \text{spin-down at } x_{ij} \\ |q_0^{11} q_1^{11}\rangle \cdots \underbrace{|00\rangle}_{x_{ij}} \cdots |q_0^{LL} q_1^{LL}\rangle & \text{empty at } x_{ij}, \end{array}$$

where we use conventional terminology letting $|q_0^{ij}\rangle$ encode *spin-up* and $|q_1^{ij}\rangle$ encode *spin-down*, say.

In the number representation of the one-particle wave function ket $|\psi\rangle$, we need consider that subset of basis states in which only one amplitude $\beta_a^{ij} = 1$ is non-zero (all other β amplitudes are zero). This subset of basis states is called the *one-particle sector*. There are $(2L)^2$ such states. So in the one-particle sector, there are two ways (interfering possibilities) for a particle to occupy the ij th lattice position

$$\beta_0^{ij} \alpha_1^{ij} |00 \cdots \underbrace{10}_{x_{ij}} \cdots 00\rangle + \alpha_0^{ij} \beta_1^{ij} |00 \cdots \underbrace{01}_{x_{ij}} \cdots 00\rangle. \quad (4)$$

Hence the occupancy probability of the ij th node is determined by first summing up the probability amplitudes of the spin-up and spin-down

basis states in the one-particle sector and then computing the resulting square of this absolute value. Letting $\gamma_{\uparrow}^{ij} \equiv \beta_0^{ij} \alpha_1^{ij}$ and $\gamma_{\downarrow}^{ij} \equiv \alpha_0^{ij} \beta_1^{ij}$, the complex probability amplitude in (2) is set equal to the sum of the two on-site probability amplitudes

$$\gamma_{ij} = \gamma_{\uparrow}^{ij} + \gamma_{\downarrow}^{ij}. \quad (5)$$

3. QUANTUM ALGORITHM TO RECOVER THE NON-LINEAR SCHRÖDINGER EQUATION IN 2+1 DIMENSIONS

To recover a macroscopic scale effective theory that approximates the Schrödinger wave equation in the long wave length limit, our quantum lattice representation of the dynamics uses the unitary \sqrt{SWAP} quantum logic gate as the collision operator that couples the on-site probability amplitudes:

$$\mathbb{C} \begin{pmatrix} \gamma_{\uparrow}^{ij} \\ \gamma_{\downarrow}^{ij} \end{pmatrix} = \frac{1}{2} \begin{pmatrix} 1-i & 1+i \\ 1+i & 1-i \end{pmatrix} \begin{pmatrix} \gamma_{\uparrow}^{ij} \\ \gamma_{\downarrow}^{ij} \end{pmatrix}, \quad (6)$$

and eight stream operators which independently shift the \uparrow and \downarrow components of the discretized spinor wave function in the $\pm\hat{x}$ and $\pm\hat{y}$ directions. The stream operator and its transpose (which is its adjoint and inverse) in the \hat{x} direction for the first (spin-up) component are:

$$S_{x\uparrow} \begin{pmatrix} \gamma_{\uparrow}^{ij} \\ \gamma_{\downarrow}^{ij} \end{pmatrix} = \begin{pmatrix} \gamma_{\uparrow}^{i+1,j} \\ \gamma_{\downarrow}^{ij} \end{pmatrix} \quad S_{x\uparrow}^T \begin{pmatrix} \gamma_{\uparrow}^{ij} \\ \gamma_{\downarrow}^{ij} \end{pmatrix} = \begin{pmatrix} \gamma_{\uparrow}^{i-1,j} \\ \gamma_{\downarrow}^{ij} \end{pmatrix}, \quad (7)$$

and the stream operators in the \hat{x} direction for the second (spin-down) component of the discretized spinor wave function:

$$S_{x\downarrow} \begin{pmatrix} \gamma_{\uparrow}^{ij} \\ \gamma_{\downarrow}^{ij} \end{pmatrix} = \begin{pmatrix} \gamma_{\uparrow}^{i,j} \\ \gamma_{\downarrow}^{i+1,j} \end{pmatrix} \quad S_{x\downarrow}^T \begin{pmatrix} \gamma_{\uparrow}^{ij} \\ \gamma_{\downarrow}^{ij} \end{pmatrix} = \begin{pmatrix} \gamma_{\uparrow}^{i,j} \\ \gamma_{\downarrow}^{i-1,j} \end{pmatrix}. \quad (8)$$

Similarly, we define the four stream operators in the \hat{y} direction:

$$S_{y\uparrow} \begin{pmatrix} \gamma_{\uparrow}^{ij} \\ \gamma_{\downarrow}^{ij} \end{pmatrix} = \begin{pmatrix} \gamma_{\uparrow}^{i,j+1} \\ \gamma_{\downarrow}^{ij} \end{pmatrix} \quad S_{y\uparrow}^T \begin{pmatrix} \gamma_{\uparrow}^{ij} \\ \gamma_{\downarrow}^{ij} \end{pmatrix} = \begin{pmatrix} \gamma_{\uparrow}^{i,j-1} \\ \gamma_{\downarrow}^{ij} \end{pmatrix}. \quad (9)$$

$$S_{y\downarrow} \begin{pmatrix} \gamma_{\uparrow}^{ij} \\ \gamma_{\downarrow}^{ij} \end{pmatrix} = \begin{pmatrix} \gamma_{\uparrow}^{i,j} \\ \gamma_{\downarrow}^{i,j+1} \end{pmatrix} \quad S_{y\downarrow}^T \begin{pmatrix} \gamma_{\uparrow}^{ij} \\ \gamma_{\downarrow}^{ij} \end{pmatrix} = \begin{pmatrix} \gamma_{\uparrow}^{i,j} \\ \gamma_{\downarrow}^{i,j-1} \end{pmatrix}. \quad (10)$$

We define the fundamental evolution operator for direction $\hat{w} = \hat{x}$ or \hat{y} and spin $\sigma = \uparrow$ or \downarrow as follows:

$$\mathcal{U}_{w\sigma} = S_{w\sigma} \mathcal{C}. \quad (11)$$

Now we define the *interleaved evolution operator* (which would be identity if the stream and collide operators commuted) as follows:

$$\mathcal{F}_{w\sigma} \equiv S_{w\sigma}^\dagger \mathcal{U}_{w\sigma}^\dagger S_{w\sigma} \mathcal{U}_{w\sigma} \quad (12a)$$

$$= S_{w\sigma}^\dagger \mathcal{C}^\dagger S_{w\sigma} \mathcal{C} \quad (12b)$$

$$= S_{w\sigma}^T \mathcal{C} S_{w\sigma} \mathcal{C} \quad (12c)$$

$$= S_{-w,\sigma} \mathcal{C} S_{w\sigma} \mathcal{C}, \quad (12d)$$

since the adjoint of the fundamental evolution operator is $\mathcal{U}_{w\sigma}^\dagger = \mathcal{C}^\dagger S_{w\sigma}^\dagger$, the stream operator is real $S_{w\sigma}^\dagger = S_{w\sigma}^T$, and the collide operator is self-adjoint $\mathcal{C}^\dagger = \mathcal{C}$. Because of the spacetime interpretation of spin,⁽⁸⁾ where if spin-up moves along \hat{w} say then spin-down moves along $-\hat{w}$, then the interleaved evolution operator is invariant under the following simultaneous spin flip and spatial inversion:

$$\mathcal{F}_{-w,-\sigma} = \mathcal{F}_{w\sigma}. \quad (13)$$

For example, $\mathcal{F}_{-x,\uparrow} = \mathcal{F}_{x\downarrow}$.

Now, let E denote the local quantum evolution operator that advances the discretized spinor wave function one unit in time. Then the evolution equation is the following:

$$\begin{pmatrix} \gamma_\uparrow^{i,j}(t + \Delta t) \\ \gamma_\downarrow^{ij}(t + \Delta t) \end{pmatrix} = E \begin{pmatrix} \gamma_\uparrow^{i,j}(t) \\ \gamma_\downarrow^{ij}(t) \end{pmatrix} \quad (14)$$

The evolution operator can be partitioned in space using an operator splitting method. A third-order accurate quantum algorithm for the local evolution operator has the form

$$E = \mathcal{F}_{-y\downarrow} \mathcal{F}_{y\uparrow} \mathcal{F}_{-x\uparrow} \mathcal{F}_{x\downarrow} \quad (15)$$

where the macroscopic effective field theory for the spinor field $\psi = \begin{pmatrix} \gamma_\uparrow \\ \gamma_\downarrow \end{pmatrix}$ is

$$\partial_t \psi = \frac{i}{2} \frac{\Delta x^2}{\Delta t} \sigma_x (\partial_{xx} + \partial_{yy}) \psi + \mathcal{O}(\epsilon^3), \quad (16)$$

where $\sigma_x = \begin{pmatrix} 0 & 1 \\ 1 & 0 \end{pmatrix}$ and where $\epsilon \sim \Delta x \sim \sqrt{\Delta t}$. So if we trace over the spin components of ψ and form the scalar $\Psi \equiv \gamma_\uparrow + \gamma_\downarrow$, we obtain the following non-relativistic wave equation for a free quantum particle:

$$\partial_t \Psi = i \frac{\hbar}{2m} (\partial_{xx} + \partial_{yy}) \Psi + \mathcal{O}(\epsilon^3), \tag{17}$$

where the diffusion constant associated with the particle mass is $(\hbar/m = \Delta x^2/\Delta t)$ in lattice units. Quadratic products of the interleaved evolution operator (12) are invariant to order ϵ^3 under the following double spin flip and spatial interchange operation:

$$\mathcal{F}_{w,\sigma} \mathcal{F}_{w',\sigma'} = \mathcal{F}_{w',-\sigma'} \mathcal{F}_{w,-\sigma} + \mathcal{O}(\epsilon^3). \tag{18}$$

For example, $\mathcal{F}_{x\uparrow} \mathcal{F}_{y\downarrow} = \mathcal{F}_{y\uparrow} \mathcal{F}_{x\downarrow}$ and $\mathcal{F}_{x\uparrow} \mathcal{F}_{y\uparrow} = \mathcal{F}_{y\downarrow} \mathcal{F}_{x\downarrow}$. Hence using (18), there are $\binom{4}{2} = 6$ ways to re-order the spatial indices of the evolution operator (15). Then, using (13), for each configuration of the spatial indices there are 16 ways to re-order the spin indices of (15). Hence, there are a total of 96 ways to rewrite the quantum algorithm (15). For example, we can rewrite (15):

$$E \stackrel{(13)}{=} \mathcal{F}_{y\uparrow} \mathcal{F}_{y\uparrow} \mathcal{F}_{x\downarrow} \mathcal{F}_{x\downarrow} \tag{19a}$$

$$\stackrel{(18)}{=} \mathcal{F}_{y\uparrow} \mathcal{F}_{x\uparrow} \mathcal{F}_{y\downarrow} \mathcal{F}_{x\downarrow} \tag{19b}$$

$$\stackrel{(18)}{=} \mathcal{F}_{x\uparrow} \mathcal{F}_{x\uparrow} \mathcal{F}_{y\downarrow} \mathcal{F}_{y\downarrow}. \tag{19c}$$

Every version has the same algorithmic complexity and the error terms are always order ϵ^3 . Furthermore, there are versions of the quantum algorithm where the error terms differ only by an overall sign change. We exploit this feature to judiciously cause a cancellation of all ϵ^3 error terms by using twice as many operators. This doubles the algorithmic complexity, but the error is then pushed out to fourth-order. Although the algorithmic complexity increases by a factor of 2, the numerical accuracy of the algorithm increases by a factor of 4 because of the diffusive ordering of the space and time fluctuations (because (17) is parabolic). Therefore, it is advantageous to employ this numerical schema.

As a case in point, the error terms in (19a) and in (19c) differ only by an overall sign. Hence, choosing our evolution operator to be

$$E = \mathcal{F}_{x\uparrow}^2 \mathcal{F}_{y\downarrow}^2 \mathcal{F}_{y\uparrow}^2 \mathcal{F}_{x\downarrow}^2, \tag{20}$$

we recover the following macroscopic effective field theory for the spinor field

$$\partial_t \psi = i \frac{\Delta x^2}{\Delta t} \sigma_x (\partial_{xx} + \partial_{yy}) \psi + \mathcal{O}(\epsilon^4). \tag{21}$$

Again, tracing over the spin degrees of freedom, we obtain the Schrödinger wave equation as our effective field theory, but now with diffusion constant

$$\frac{\hbar}{m} = 2 \frac{\Delta x^2}{\Delta t}. \tag{22}$$

We add a potential V by rotating the overall phase of the spinor field following each application of (20)

$$\psi(t + \Delta t) = E e^{-i\Delta t V/\hbar} \psi(t) \tag{23}$$

$$\stackrel{(22)}{=} E e^{-i\Delta x^2 (2m/\hbar^2) V} \psi(t). \tag{24}$$

The resulting equation of motion is

$$\partial_t \psi = i \frac{\Delta x^2}{\Delta t} \sigma_x (\partial_{xx} + \partial_{yy}) \psi - \frac{i}{\hbar} V \psi + \mathcal{O}(\epsilon^4), \tag{25}$$

or in terms of the scalar wave function

$$i \hbar \partial_t \Psi = -\hbar \frac{\Delta x^2}{\Delta t} (\partial_{xx} + \partial_{yy}) \Psi + V \Psi + \mathcal{O}(\epsilon^4). \tag{26}$$

The addition of the potential does not introduce any greater error nor diminishes the numerical accuracy of the scheme. Using (13), there are 2^8 ways to rewrite (20). Furthermore, (20) must be invariant under an interchange of the spatial labels x and y and the spin labels \uparrow and \downarrow . Hence, there are at least 256 ways of writing a quantum algorithm that is fourth-order accurate.

4. TRANSVERSE INSTABILITY

For convenience, we briefly review some properties of a 1D soliton wave train solution of (1).⁽¹⁾ A planar 1D bright soliton solution of (1) is

$$\psi_0(x, t) = \phi(x - x_0 - 2vt; \beta) e^{i(vx - v^2t + \beta t + \theta)}, \tag{27}$$

where the standard soliton shape is given by

$$\phi(x; \beta) = \beta^{1/2} \operatorname{sech}(\beta^{1/2} x) \quad (28)$$

The location of the soliton wave train is x_0 , 2ν is the (transverse) soliton wave train speed, β controls its amplitude and θ its phase. For a linear stability analysis of this 1D soliton wave train, one considers perturbations of the form

$$\delta\psi(x, y, t) = [u(x) + iw(x)]e^{i\beta t + \Gamma t + ipy}, \quad (29)$$

where p is the transverse perturbation wavenumber in the y -direction, and $\Gamma(p)$ is the linear growth rate of the perturbation. An analytic solution to this linear perturbation problem does not exist, and one must resort to asymptotic theory—either about the long wavelength limit ($p=0$) or about the maximum growth rate wavenumber p_c where $\Gamma(p_c)=0$. Here, we shall consider the linear instability in the long wavelength limit, $p \ll 1$. In this limit, it can be shown⁽¹⁾ that the resulting eigenvalue problem has

$$u(x) = 0 \quad w(x) = \phi(x). \quad (30)$$

In the long wavelength limit, the transverse modulation will break up the 1D soliton wave train into N filaments, where

$$N = \frac{pL_y}{2\pi}. \quad (31)$$

5. NUMERICAL PREDICTIONS FOR NLS EQUATION IN 2+1 DIMENSIONS

We apply our quantum lattice algorithm to the solution of the NLS equation in 2+1 dimensions, using a 1024×1024 spatial grid with a soliton wave train speed $\nu=0.05$ and amplitude $\beta^{1/2}=0.085$ for three cases presented below: an unperturbed soliton wave train, a soliton wave train with an additional transverse modulation, and the interaction of two perpendicularly directed soliton wave trains.

To test whether (classical) floating-point roundoff will trigger the transverse instability in the quantum lattice algorithm we the propagation of the planar 1D bright soliton solution in the NLS equation in 2+1 dimensions. We find even after 10,000 lattice time steps there is no triggering of the transverse modulation instability, and the 1D soliton train

propagates undistorted through the lattice, see Fig. 1. The quantum algorithm is numerically stable. This is verified in the simulations for $t=0\Delta t$, $t=5\text{K}\Delta t$, $t=10\text{K}\Delta t$. The simulation error in soliton speed after 10K iterations is only 0.5% (about 5 lattice grid points on the 1024 grid).

A transverse perturbation of the form of (29) with wavenumber $p=2\pi N/L_y$, $N=8$ with an amplitude that is a factor of 10^{-7} below the initial wave train amplitude. The asymptotic linear stability predicts that the 1D soliton train should break up into 8 filamentary structures, an unstable phase, as shown in Fig. 2. This is indeed found in our simulations, with the filamentary structures becoming so isolated and peaked that the steep gradient of the wave function cannot be resolved on the grid after about $t=2100\Delta t$ iterations, even on using a 1024×1024 lattice.

Finally, we consider the interaction of two perpendicularly directed soliton wave trains. No initial perturbations are needed due to the “overlap” region of the two wave trains. A very rapid instability is immediately triggered at the intersection region of the two wave trains, and its localization and peak are so rapid that the gradient of the wave function cannot be further resolved on the grid after just 35 time steps. The instability occurs only at the point of intersection of the two soliton trains and the unaffected regions of both soliton trains propagate in normal fashion. This expected behaviour is observed in the simulation shown in Fig. 3.

6. CONCLUSION

Presented was a lattice-based quantum algorithmic method to numerically model time-dependent solutions of the Schrödinger wave equation in an arbitrary number of spatial dimensions using a fourth-order accurate operator splitting method. Here, we tested the method in 2+1 dimensions using a quantum system with a non-linear potential. Generalization to 3+1 dimensions is straightforward. This was the first numerical test of the quantum lattice gas algorithm in multiple spatial dimensions—all previous simulation results that have appeared in the literature have been for 1+1 dimensional cases. Furthermore, we probed to determine if the quantum algorithm was cable of accurately modelling the expected physical behaviour of the non-linear quantum system by triggering the onset of strong and rapid non-linear instabilities in solitary wave trains. This was a stringent test of the method.

In all the cases, the quantum algorithm performed excellently with the numerical results in perfect agreement with the theoretical predictions. Ultimately, in tracking the late time developed of the growth of the instabilities, we were limited by our fixed grid resolution. To follow

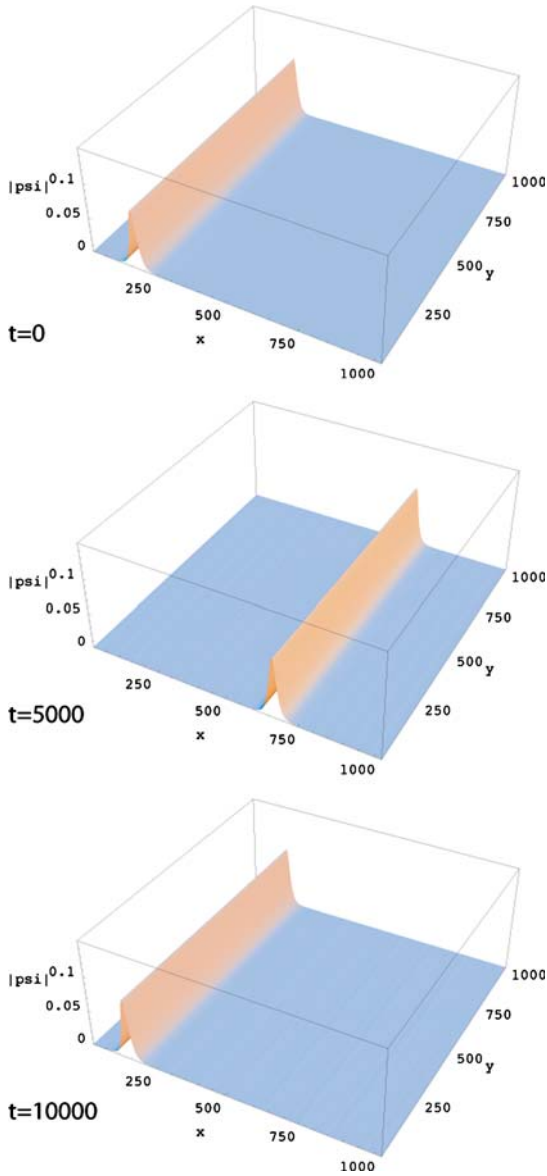


Fig. 1. Evolution of a 1D soliton wave train for the NLS equation in 2+1 dimensions on a 1024^2 grid with periodic boundary conditions. No transverse modulation instabilities are triggered, even after 10,000 iterations. By $t = 10,000\Delta t$ (bottom), the wave train has wrapped around the grid.

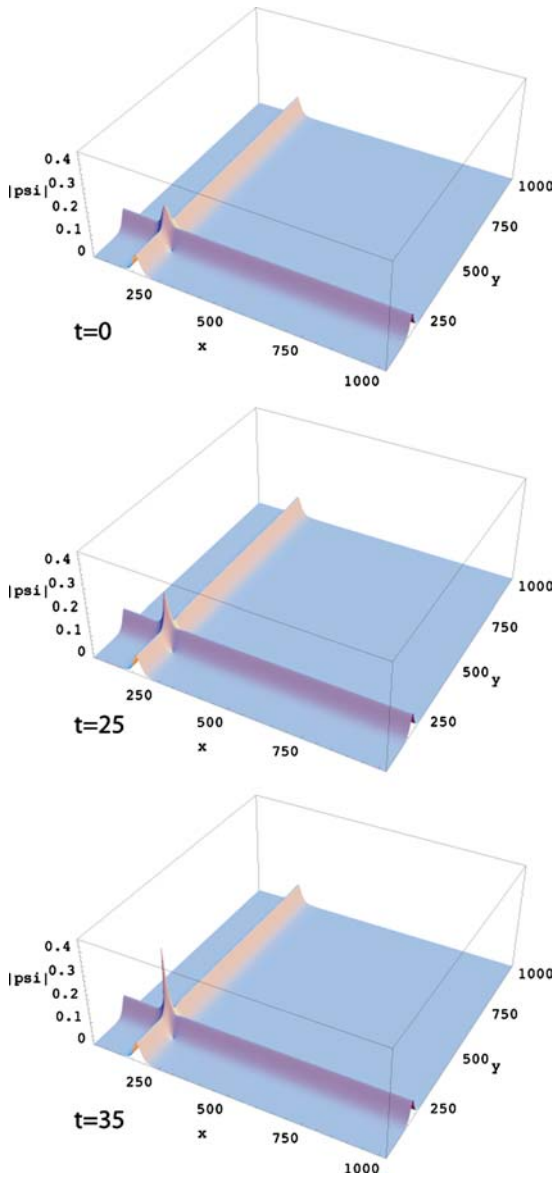


Fig. 2. Evolution of a 1D soliton wave train for the NLS equation in 2+1 dimensions on a 1024^2 grid (only half the grid is shown) with a transverse perturbation with amplitude 10^{-7} lower than the initial peak amplitude of the soliton wave train. A transverse modulation instability is triggered, clearly observable after $t = 2000\Delta t$ time steps.

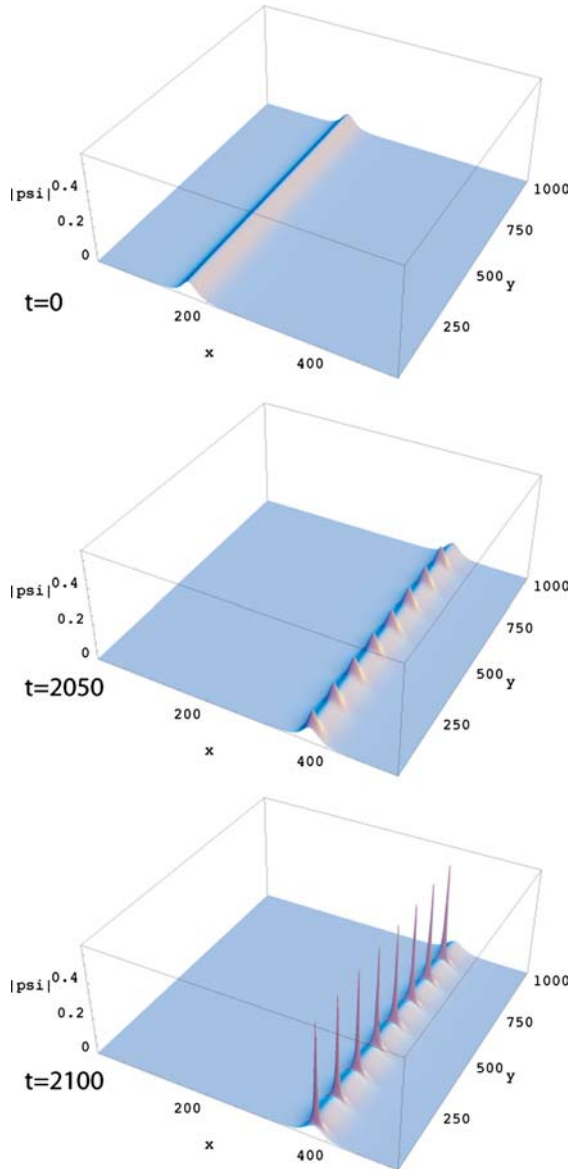


Fig. 3. Evolution of two orthogonally directed 1D soliton wave trains for the NLS equation in 2+1 dimensions on a 1024^2 grid. An rapid instability is immediately triggered, creating a rising peak at the intersection point of the solitons that reached the grid resolution after $t = 35\Delta t$ time steps.

the quantum evolution for significantly longer periods of time following the onset of a non-linear instability, one could introduce adaptive mesh refinements into our quantum algorithmic scheme, and this will be left for future work.

ACKNOWLEDGMENT

The authors wish to express their indebtedness for the support provided through the Computational Mathematics Program of the Air Force Office of Scientific Research for algorithm development research.

REFERENCES

1. Y. S. Kivshar and G. P. Agrawal, *Optical Solitons* (Academic Press, New York, 2003).
2. E. Infeld and G. Rowlands, *Nonlinear Waves, Solitons, and Chaos*, 2nd ed. (Cambridge University Press, Cambridge, 2000).
3. M. H. Jakubowski, K. Steiglitz, and R. Squier, *Phys. Rev. E* **58**, 6752 (1998).
4. M. H. Jakubowski, K. Steiglitz, and R. Squier, *Multiple-Valued Logic* **6**, 439 (2001).
5. Jeffrey Yepez, and Bruce Boghosian, *Comput. Phys. Commun.* **146**(3), 280–294 (2002).
6. George Vahala, Linda Vahala, and Jeffrey Yepez, *Phys. Lett. A* **310**, 187–196 (2003).
7. George Vahala, Linda Vahala, and Jeffrey Yepez, *Philosop. Trans. R. Soc.* **362**(1821), 1677–1690 (2004).
8. Jeffrey Yepez, *Quantum Information Processing* (6), (2005) (in press).
9. Marco Pravia, Zhiying Chen, Jeffrey Yepez, and David G. Cory, *Comput. Phys. Commun.* **146**(3), 339–344 (2002).
10. Marco Pravia, Zhiying Chen, Jeffrey Yepez, and David G. Cory, *Quantum Information Processing* **2**, 1–19 (2003).
11. Lisa C. Siskind, Bruce E. Hammer, Nelson L. Christensen, and Jeffrey Yepez, *Quantum Information Processing* **4**(6) (2005). Appearing in this special issue of QIP.